

Supporting Information

Acidity constant and DFT-based modelling of pH-responsive alendronate loading and releasing on propylamine modified silica surface

Khalid Ahmed, Shaukatali Najikhan Inamdar, Nashiour Rohman and Adam A. Skelton*

Department of Pharmaceutical Sciences, University of KwaZulu-Natal, Durban 4000, South Africa

*Corresponding author: dradamskelton@gmail.com, Tel.: +44 7507243294

S1. Distribution of mole fractions

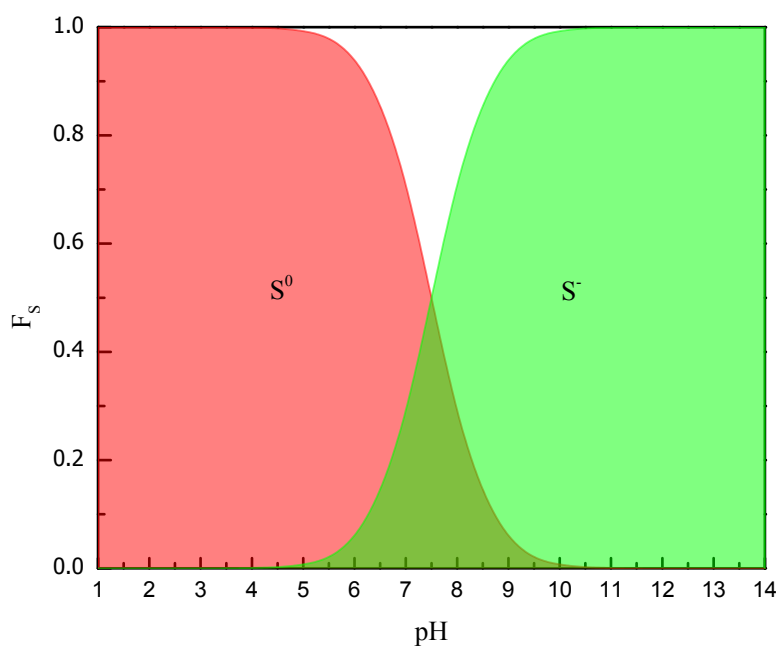
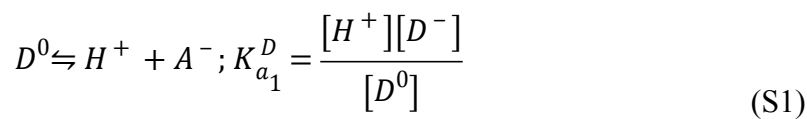


Figure S1: The variations of mole fractions of neutral and deprotonated form of silica with pH.



$$D^- \rightleftharpoons H^+ + D^{2-}; K_{a_2}^D = \frac{[H^+][D^{2-}]}{[D^-]} \quad (S2)$$

$$D^{2-} \rightleftharpoons H^+ + D^{3-}; K_{a_3}^D = \frac{[H^+][D^{3-}]}{[D^{2-}]} \quad (S3)$$

$$D^{3-} \rightleftharpoons H^+ + D^{4-}; K_{a_4}^D = \frac{[H^+][D^{4-}]}{[D^{3-}]} \quad (S4)$$

$$\begin{aligned} a_T &= [D^0] + [D^-] + [D^{2-}] + [D^{3-}] + [D^{4-}] \\ &= [A^0] \left\{ 1 + \frac{K_{a_1}^D}{[H^+]} + \frac{K_{a_1}^D K_{a_2}^D}{[H^+]^2} + \frac{K_{a_1}^D K_{a_2}^D K_{a_3}^D}{[H^+]^3} + \frac{K_{a_1}^D K_{a_2}^D K_{a_3}^D K_{a_4}^D}{[H^+]^4} \right\} \\ &= [D^0] F \end{aligned} \quad (S5)$$

where

$$F = 1 + \frac{K_{a_1}^D}{[H^+]} + \frac{K_{a_1}^D K_{a_2}^D}{[H^+]^2} + \frac{K_{a_1}^D K_{a_2}^D K_{a_3}^D}{[H^+]^3} + \frac{K_{a_1}^D K_{a_2}^D K_{a_3}^D K_{a_4}^D}{[H^+]^4} \quad (S6)$$

If F_{D^0} , F_{D^-} , $F_{D^{2-}}$, $F_{D^{3-}}$ and $F_{D^{4-}}$ are fractions of D^0 , D^- , D^{2-} , D^{3-} and D^{4-} , they can be rearranged as:

$$F_{D^0} = \frac{1}{F}; F_{D^-} = \frac{K_{a_1}^D}{[H^+]} \frac{1}{F}; F_{D^{2-}} = \frac{K_{a_1}^D K_{a_2}^D}{[H^+]^2} \frac{1}{F}; F_{D^{3-}} = \frac{K_{a_1}^D K_{a_2}^D K_{a_3}^D}{[H^+]^3} \frac{1}{F}; F_{D^{4-}} = \frac{K_{a_1}^D K_{a_2}^D K_{a_3}^D K_{a_4}^D}{[H^+]^4} \frac{1}{F} \quad (S7)$$

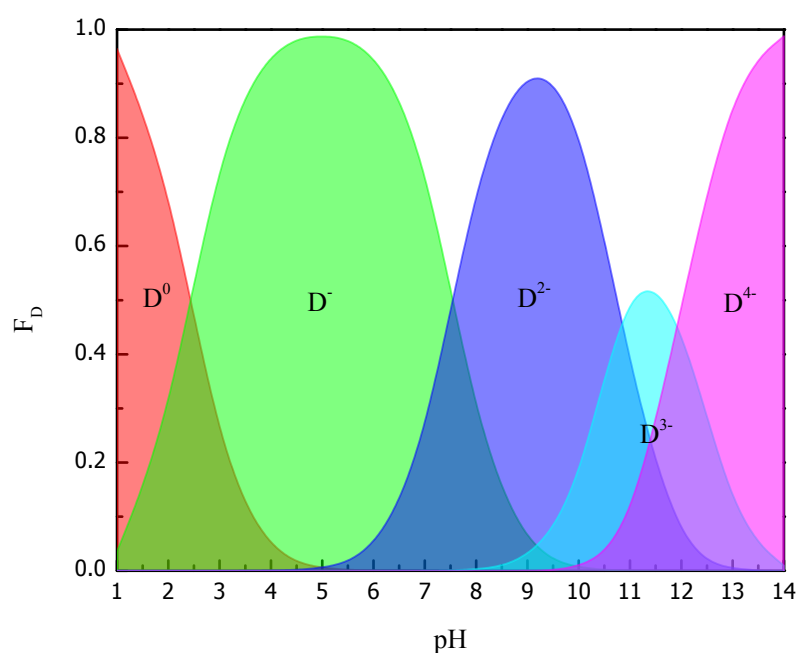


Figure S2: The variations of mole fractions of neutral and deprotonated drug with pH.

The fractions of various combinations of SD with pH is shown in Figure S3 It shows that there is a higher fraction of S^0D^0 and S^0D^- in the range of $pH < 7$, whereas S^-D^{2-} , S^-D^{3-} , and S^-D^{4-} dominates in the range of $pH > 7$. In the mid pH range, small contribution comes from S^0D^{2-} and S^-D^- . However, contributions from S^0D^{3-} , S^0D^{4-} and S^-D^0 are too small to be detected.

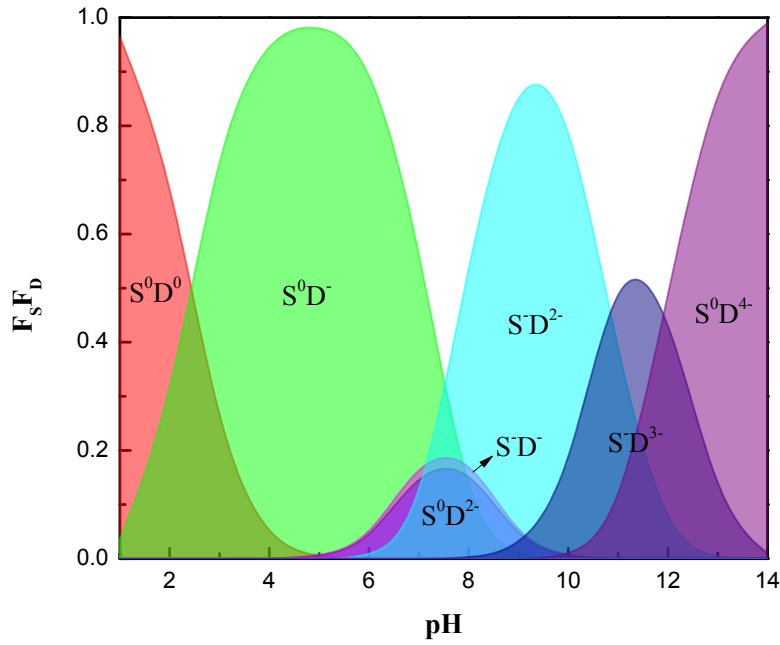
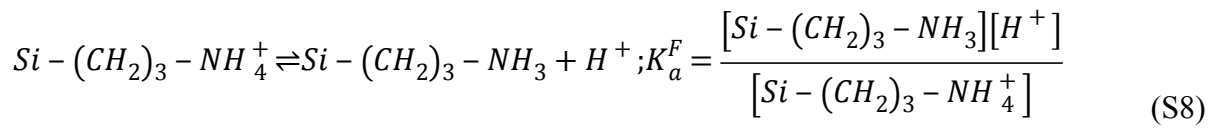


Figure S3: The variations of product of mole fractions of silica and drug with pH.



$$F_{F^0} = \frac{1}{1 + 10^{pK_a^F - pH}}; F_{F^+} = 1 - F_{F^0} \quad (S9)$$

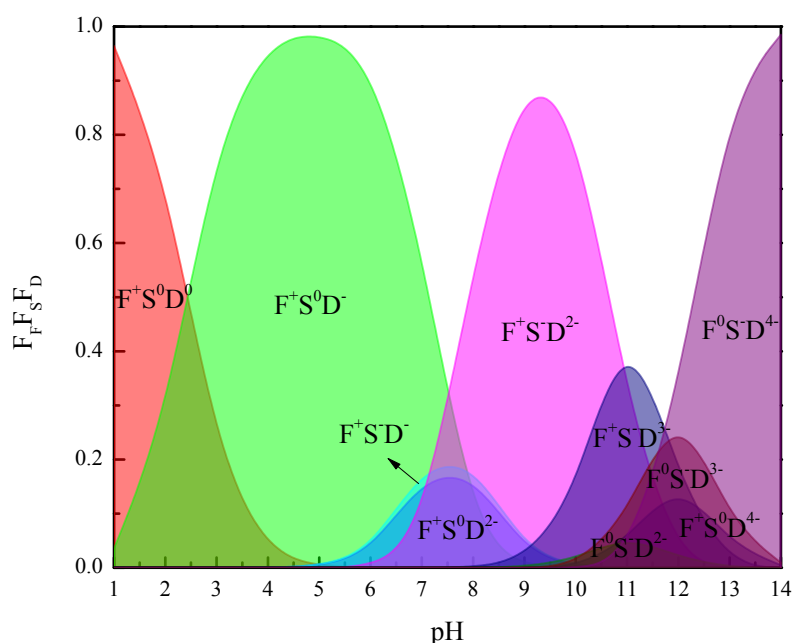


Figure S4: The variations of product of mole fractions of functional group, silica and drug with pH.

S2. Geometry optimization

To study the interaction of D^0 molecule with S^0 silica surface, we have placed D^0 molecule both horizontally (Figure S5A and S5B) and vertically (Figure S5C and S5D) on silica surface. It is found that vertical position (Figure S5C) that allows maximum H-bonding between bisphosphonates and SiOH favours the most stable configuration ($E = 5.69 \text{ kCal.mol}^{-1}$). Five possible states of the drug molecule (D^0 , D^- , D^{2-} , D^{3-} and D^{4-}) were considered and placed in four possible positions on top of silica surfaces as shown in Figure 3.

The geometry optimization of silica (S^0 and S^-) and propylamine functionalized silica (F^+S^0 , F^+S^- , F^0S^0 , F^0S^-) were carried out. The resultant optimization energies are shown in Figure S5. Figure S5 shows that the positively charged functional group has more negative energy than the neutral functional group. Ten different geometry optimisation for $S^0D^0F^0$ and $S^0D^0F^+$ are shown in Figures S6 and S7. The interaction energy is with incorporation of propylamine on

silica surface. The alendronate molecule is tilted around propylamine group (Figure S5C) favouring both H-bonding and hydrophobic interactions.

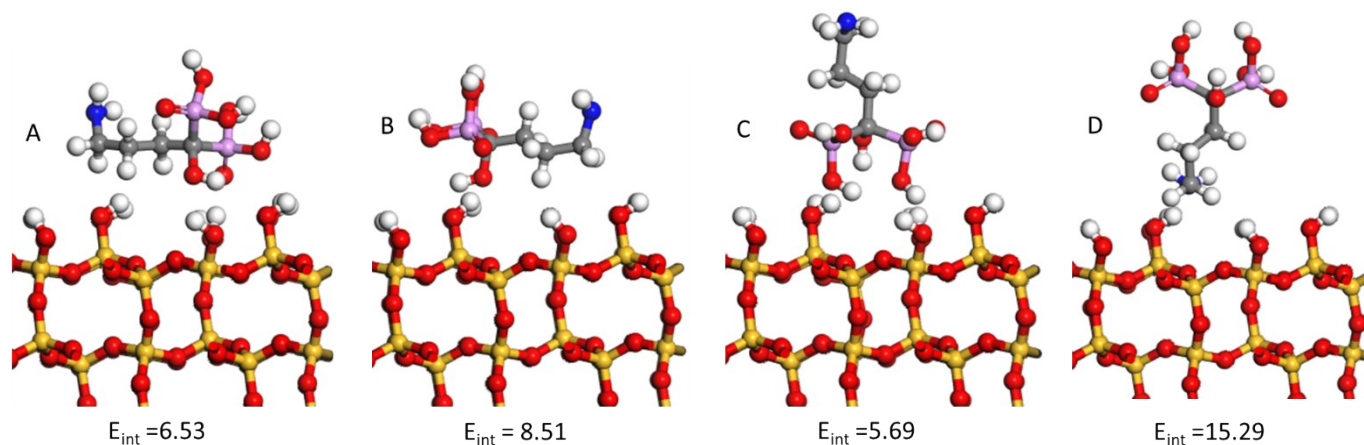


Figure S5: Lowest energy configurations of drug (D^0) on silica surface (S^0) at different position.

The corresponding interaction energies, E in kcal.mol^{-1} are given below.

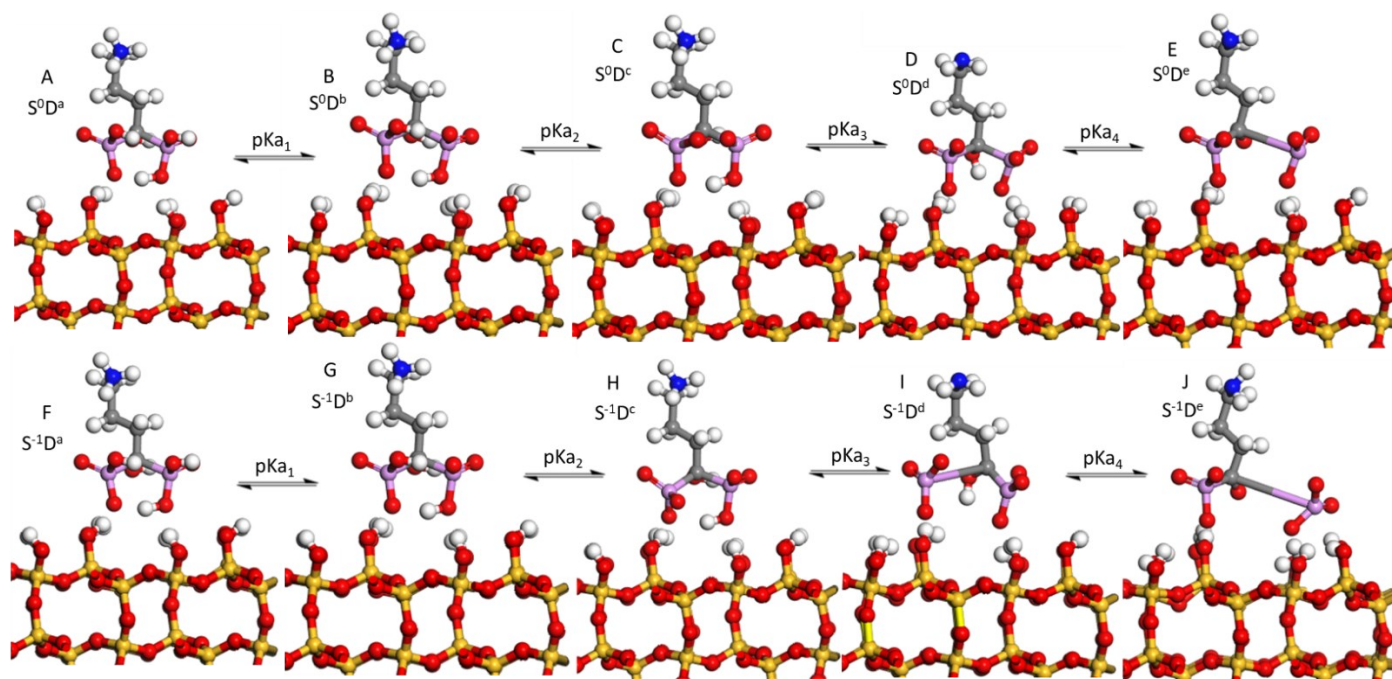


Figure S6: Lowest energy configurations of neutral and deprotonated silica surface with drug molecule with different charged state.

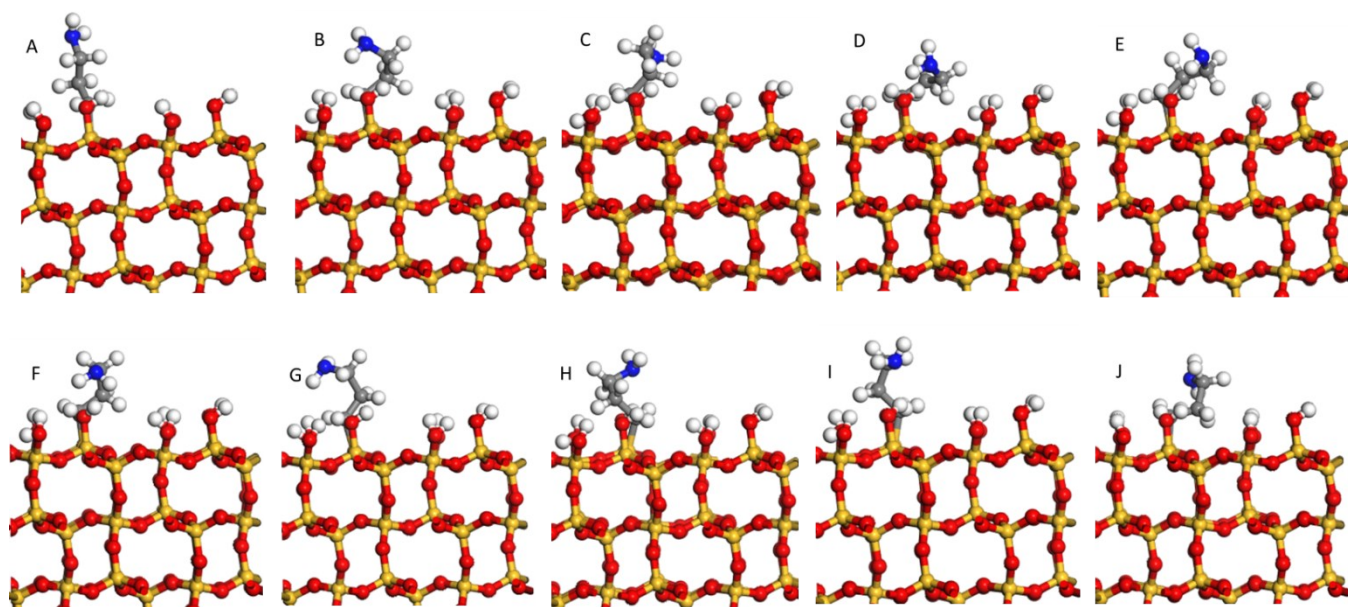


Figure S7: Optimization of neutral propylamine functionalized silica in ten different positions.

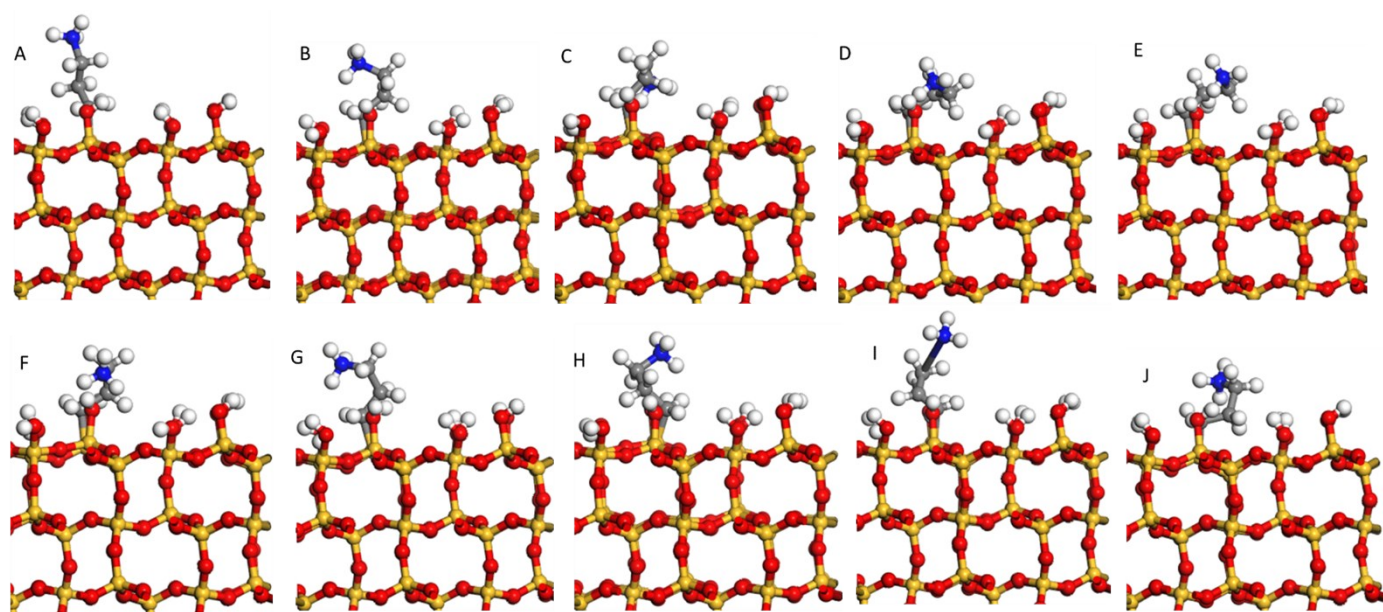


Figure S8: Optimization of positively charged propylamine functionalized silica in ten different positions.

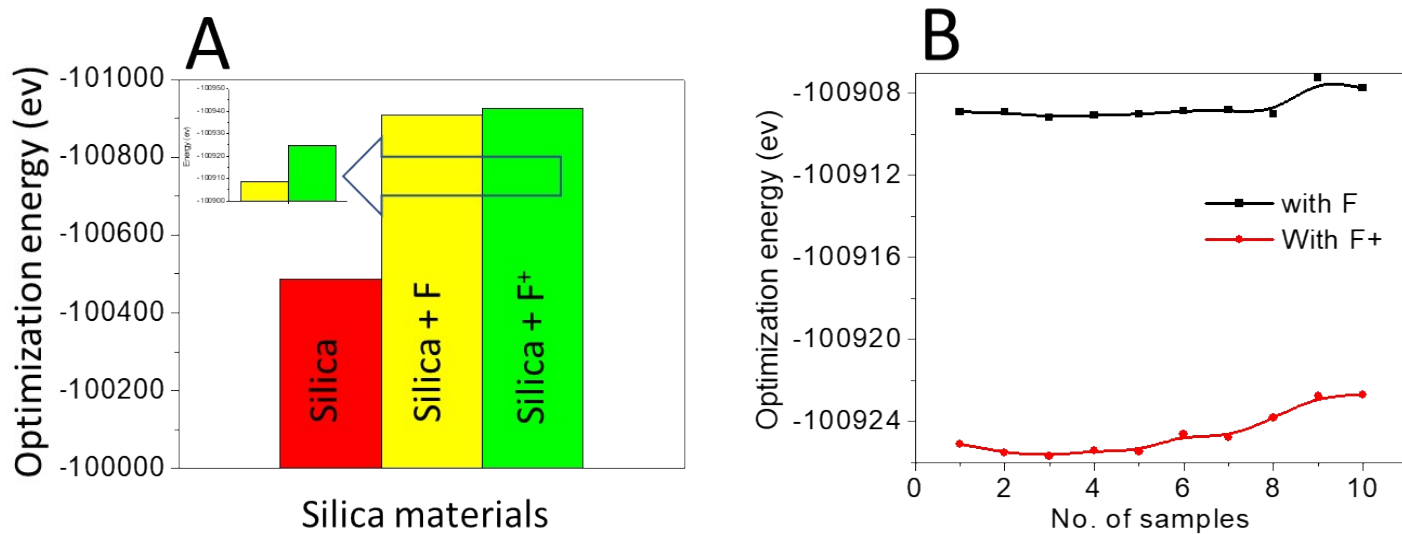


Figure S9: Optimization energies for silica surface in presence of protonated (F⁺) and neutral (F⁰) functional group.

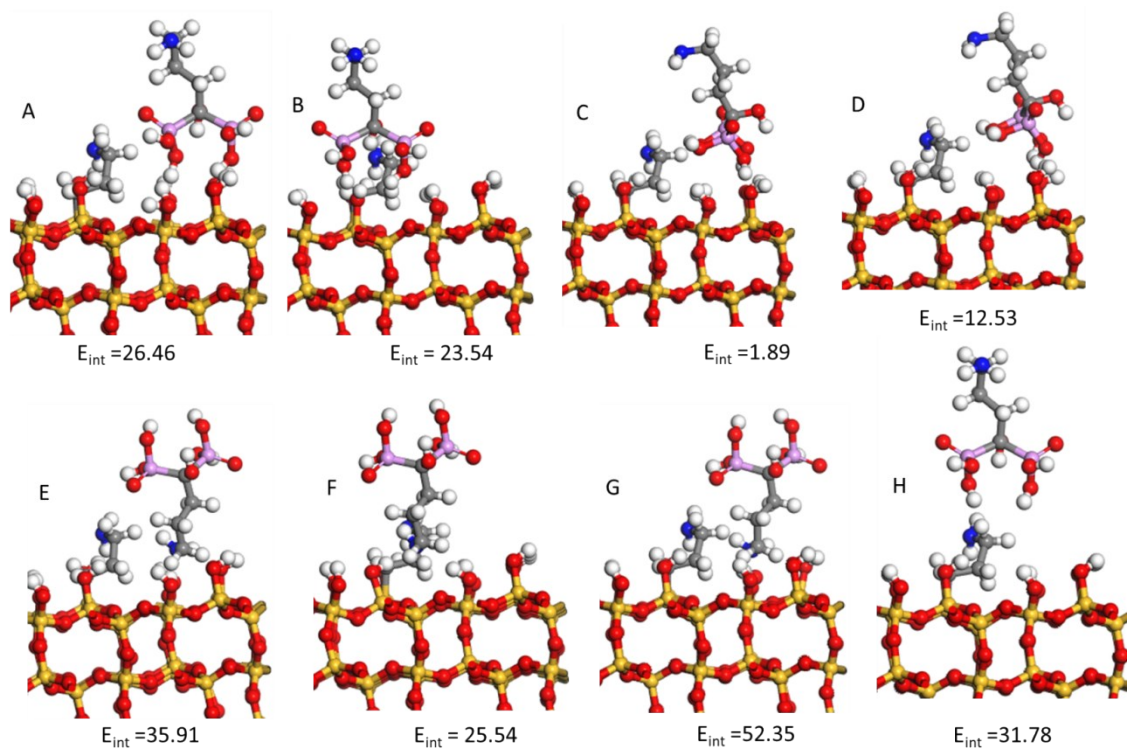


Figure S10: Lowest energy configurations for all combinations of silica (S^0) with a functional group and with drug (D^0) in different position

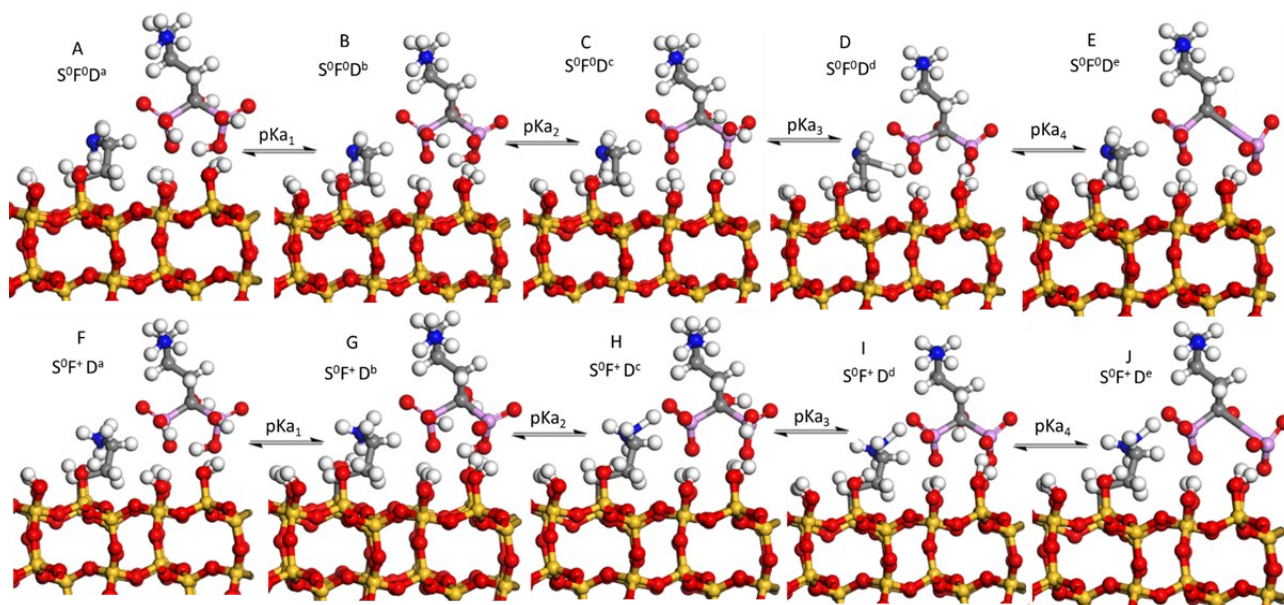


Figure S11: The lowest energy configurations for the combinations of neutral silica (S^0) in presence of neutral (F^0) and protonated (F^+) functional group with the different neutral and deprotonated states of the drug.

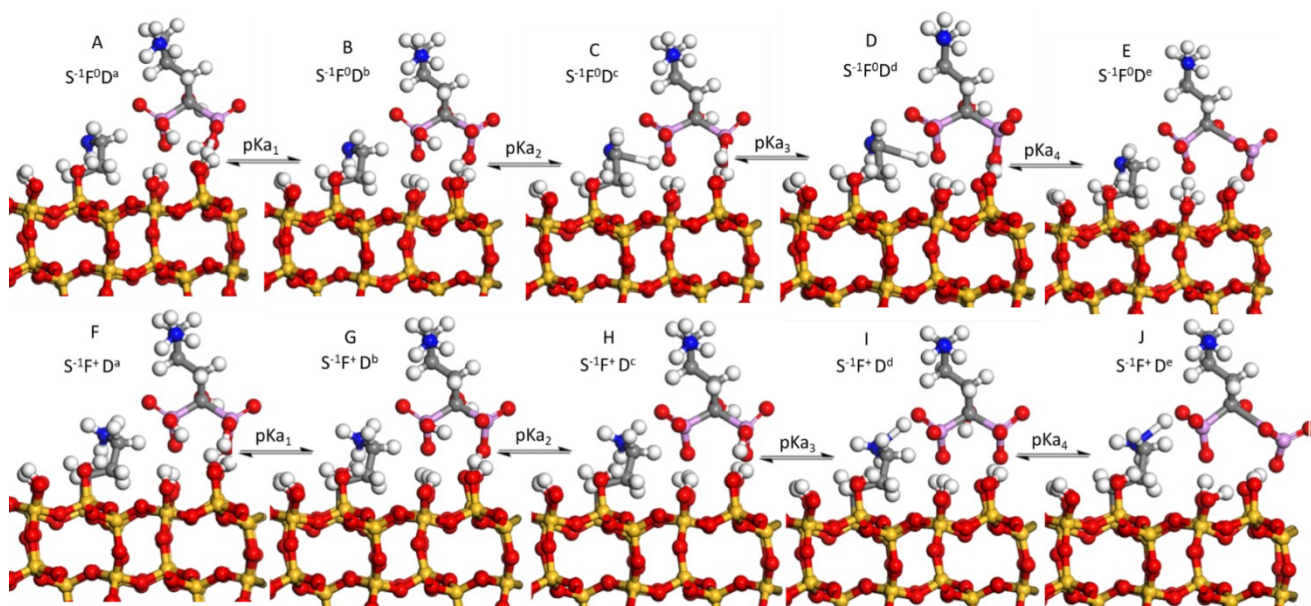


Figure S12: The lowest energy configurations for the combinations of deprotonated silica (S^-) in presence of neutral (F^0) and protonated (F^+) functional group with the different neutral and deprotonated states of drug.

References

1. J, C.S., et al., *First principles methods using CASTEP*. Zeitschrift Für Krist. - Cryst. Mater, 2005. **220**.
2. Perdew, J.P., K. Burke, and M. Ernzerhof, *Generalized Gradient Approximation Made Simple*. Phys Rev Lett, 1996. **77**(18): p. 3865-3868.
3. Meyer, B., H. Rabaa, and D. Marx, *Water adsorption on ZnO(1010): from single molecules to partially dissociated monolayers*. Phys. Chem. Chem. Phys., 2006. **8**: p. 8.
4. Vanderbilt, D., *Soft self-consistent pseudopotentials in a generalized eigenvalue formalism*. Phys. Rev. B, 1990. **41**: p. 5.